NGC 922 – a new drop-through ring galaxy[*]

O. I. Wong,[1,2,3]† G. R. Meurer,[2] K. Bekki,[4] D. J. Hanish,[2] R. C. Kennicutt,[5]
J. Bland-Hawthorn,[6] E. V. Ryan-Weber,[7] B. Koribalski,[3] V. A. Kilborn,[3,8]
M. E. Putman,[9] J. S. Heiner,[10,11] R. L. Webster,[1] R. J. Allen,[11] M. A. Dopita,[12]
M. T. Doyle,[13] M. J. Drinkwater,[13] H. C. Ferguson,[11] K. C. Freeman,[12] T. M. Heckman,[2]
C. Hoopes,[2] P. M. Knezek,[14] M. J. Meyer,[11] M. S. Oey,[9] M. Seibert,[15] R. C. Smith,[16]
L. Staveley-Smith,[3] D. Thilker,[2] J. Werk[9] and M. A. Zwaan[17]

[1]*School of Physics, University of Melbourne, VIC 3010, Australia*
[2]*Department of Physics and Astronomy, Johns Hopkins University, Baltimore, MD 21211, USA*
[3]*Australia Telescope National Facility, CSIRO, PO Box 76, Epping, NSW 1710, Australia*
[4]*School of Physics, University of New South Wales, Sydney, NSW 2052, Australia*
[5]*Steward Observatory, University of Arizona, 933 North Cherry Avenue, Tucson, AZ 85721, USA*
[6]*Anglo-Australian Observatory, PO Box 296, Epping, NSW 2121, Australia*
[7]*Institute of Astronomy, Madingley Road, Cambridge CB3 0HA*
[8]*Centre for Astrophysics & Supercomputing, Swinburne University of Technology, PO Box 218, Hawthorn, VIC 3122, Australia*
[9]*Department of Astronomy, University of Michigan, 830 Dennison Building, Ann Arbor, MI 48109-1042, USA*
[10]*Kapteyn Astronomical Institute, University of Groningen, PO Box 800, 9700 AV Groningen, the Netherlands*
[11]*Space Telescope Science Institute, 3700 San Martin Drive, Baltimore, MD 21218, USA*
[12]*Research School of Astronomy and Astrophysics, Australian National University, Cotter Road, Weston Creek, ACT 2611, Australia*
[13]*Deparment of Physics, University of Queensland, QLD 4072, Australia*
[14]*WIYN, Inc., 950 North Cherry Avenue, Tucson, Arizona, USA*
[15]*California Institute of Technology, MC 405-47, 1200 East California Boulevard, Pasadena, CA 91125, USA*
[16]*Cerro Tololo Inter-American Observatory (CTIO), Casilla 603, La Serena, Chile*
[17]*European Southern Observatory, Karl-Schwarzschild-Str. 2, 85748 Garching b. München, Germany*

ABSTRACT

We have found the peculiar galaxy NGC 922 to be a new drop-through ring galaxy using multiwavelength (ultraviolet–radio) imaging and spectroscopic observations. Its 'C'-shaped morphology and tidal plume indicate a recent strong interaction with its companion which was identified with these observations. Using numerical simulations we demonstrate that the main properties of the system can be generated by a high-speed off-axis drop-through collision of a small galaxy with a larger disc system, thus making NGC 922 one of the nearest known collisional ring galaxies. While these systems are rare in the local Universe, recent deep *Hubble Space Telescope* images suggest they were more common in the early Universe.

Key words: galaxies: individual: NGC 922 – Galaxy: structure.

1 INTRODUCTION

Interests in ring galaxies as examples of galaxy collisions date back to early simulations of the famous Cartwheel galaxy (Lynds & Toomre 1976), which was modelled by a small galaxy passing through a larger one. This interaction is thought to spread out stellar populations, induce star formation and thicken the disc of the larger galaxy. Here, we present observations of the peculiar galaxy NGC 922 which Block et al. (2001) describe as a dust-obscured grand design spiral. Here, we argue that it is in fact a particularly nearby example of this phenomenon and we identify its perturber.

We find striking resemblances between this galaxy and several high-redshift galaxies categorized as *clump cluster* galaxies by Elmegreen et al. (2005). Since both galaxy density and the dispersion about the Hubble flow increase with redshift, the probability of interactions between galaxies should also increase. Hence, ring galaxies should be more common in the early Universe.

Our intent in this discovery paper, is to present the available observational properties of the system, identify the companion and

---

[*]Based on observations with the NASA Galaxy Evolution Explorer (GALEX). GALEX is operated for NASA by the California Institute of Technology under NASA contract NAS5-98034.
†E-mail: iwong@physics.unimelb.edu.au

demonstrate that the system can be accounted for by an off-axis collision model. We describe our multiwavelength observations in Section 2. Section 3 presents our numerical simulations, which reproduces ring morphology of NGC 922 from simple dynamical modelling.

2 OBSERVATIONS

The Survey for Ionization in Neutral Gas Galaxies (SINGG Meurer et al. 2006) and its sister survey, the Survey of Ultraviolet emission of Neutral Gas Galaxies (SUNGG) are surveys in the Hα and ultraviolet (UV) of an HI-selected sample of galaxies from the HI Parkes All-Sky Survey (HIPASS; Meyer et al. (2004), Koribalski et al. (2004)). SINGG consists of optical *R*-band and Hα images obtained primarily from the 1.5-m telescope at Cerro Tololo Inter-American Observatory (CTIO), Chile. The Galaxy Evolution Explorer (GALEX) satellite telescope is used to obtain the far-UV (FUV) 1515-Å images and near-UV (NUV) 2273-Å images for SUNGG.

In addition, observations from the six-degree Field Galaxy Survey (6dFGS; Jones et al. 2004) and the two-Micron All-Sky Survey (2MASS; Jarrett et al. 2000) were also used.

2.1 Multiwavelength morphology and luminosity

Two Hα sources, HIPASSJ0224−24:S1 (NGC 922) and HIPASSJ0224−24:S2 (2MASXJ02243002−2444441) were identified with the SINGG data (Meurer et al. 2006). For convenience, we refer to the first source as NGC 922 and its companion as S2 in this paper. A deep grey-scale optical image of the NGC 922 field created from UK Schmidt plates, courtesy David Malin[1] is as shown in Fig. 1 where NGC 922 is located in the south-east corner and its companion is projected 8.2 arcmin (102 kpc) towards the north-west. The enlarged images of NGC 922 and S2 are colour composite images where red represents Hα, green represents *R* band and blue represents FUV. The distance of 43 Mpc to the NGC 922/S2 system was derived from the HI radial velocity, using the Mould et al. (2000) distance model and adopting a Hubble constant $H_0 = 70 \, \mathrm{km \, s^{-1} \, Mpc^{-1}}$ (Meurer et al. 2006). Young star forming regions in the ring of NGC 922 are revealed with the Hα and FUV observations. As shown clearly in the deep optical image from Fig. 1, a spray of stars (only visible in *R* band in the bottom colour image) from NGC 922 can be seen to be extending towards S2.

The Hα equivalent width (EW) profile and the radial colour profiles of NGC 922 are shown in Fig. 2. All the profiles were generated with the same isophotal parameters using the task ELLIPSE in IRAF.[2] Concentric ellipses were fitted in each image centred on the location of the NUV brightness peak. The surface brightness radial profile was then measured as a function of semimajor distance from that location. The position angle of NGC 922 is 51°. It can be seen from the Hα EW profile that the brightness peak in Hα (at 5 arcsec) is slightly displaced from the NUV brightness peak. The central colour dip corresponds to the central peaks in FUV and NUV. The two main peaks in the Hα EW profile correspond to the core of the galaxy ($R \sim 5$ arcsec) and the ring ($R \sim 50$ arcsec). Likewise, the FUV–
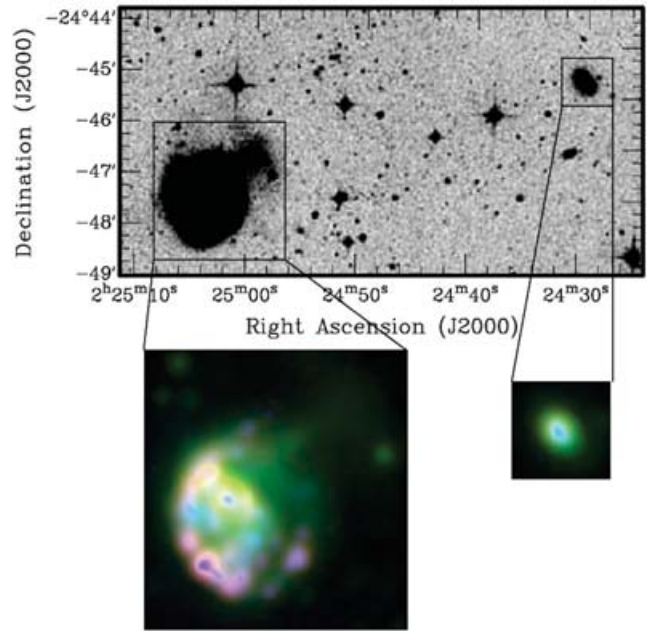

Figure 1. The grey-scale optical image (top) is a deep image from digitally stacked plates of NGC 922 (bottom left-hand side) and S2 (top right-hand side). The height of the grey-scale image is ∼4 arcmin. The enlarged images are SINGG–SUNGG composite images of NGC 922 and S2 where red represents Hα, green represents *R* band and blue represents FUV. A diffuse plume of stars on the north-western side of NGC 922 can be seen in the *R* band to be extending towards the companion.
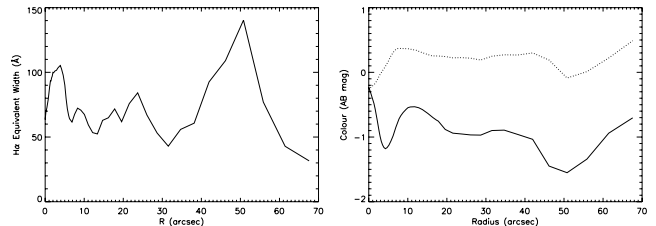

Figure 2. The Hα EW (radial) profile of NGC 922 is shown on the left-hand panel and radial colour profiles of NGC 922 are shown on the right-hand panel where the FUV–NUV and FUV − *R* colour profiles are represented by the dotted and solid lines, respectively.

NUV colour profile shows minima at these radii. Hence, star formation is enhanced in the core and especially the ring. This indicates that star formation is propagating in NGC 922. We also find the inner regions of NGC 922 to be slightly redder, presumably older, than the outer regions as shown by the FUV − *R* profile in Fig. 2, and in agreement with ring galaxy model predictions (e.g. Hernquist & Weil 1993)

The optical spectra and near-infrared (NIR) images (*JHK* bands) of NGC 922 and S2 were obtained from the 6dF Galaxy Redshift Survey (Jones et al. 2004) and the 2MASS Extended Source Catalogue (Jarrett et al. 2000), respectively. Radial velocities of NGC 922 and S2 were measured from the spectra and are as listed in Table 1. The fibre diameter of the 6dF instrument is 6.7 arcsec which translates to an aperture size of 1.4 kpc for NGC 922.

Both the NUV and FUV magnitudes were corrected for foreground Galactic reddening using the relationships of Seibert et al. (2005) based on the dust reddening maps of Schlegel, Finkbeiner & Davis (1998). The FUV attenuation (A_{FUV}) due to internal

---

[1] http://www.aao.gov.au/images/deep_html/n0922_d.html

[2] IRAF is distributed by the National Optical Astronomy Observatories, which are operated by the Association of Universities for Research in Astronomy, Inc., under cooperative agreement with the National Science Foundation.

Table 1. Observed properties of NGC 922 and S2.

Properties	NGC 922	S2
Right ascension (J2000)	02:25:04.4	02:24:30.0
Declination (J2000)	−24:47:17	−24:44:44
v_h (km s^{-1})	3077	3162
$E(B-V)_G$ (mag)	0.019	0.018
$E(B-V)_i$ (mag)	0.21	0.23
$(M_R)_0$ (AB mag)	−21.59	−18.45
(FUV–NUV)$_0$ (AB mag)	−0.09	−0.08
$(NUV-R)_0$ (AB mag)	1.52	1.32
$(R-J)_0$ (AB mag)	0.90	0.75
$(J-H)_0$ (AB mag)	0.54	0.44
$(H-K)_0$ (AB mag)	0.16	0.58
f_0(Hα) (10^{-12} erg cm^{-2} s^{-1})	4.65 ± 0.18	0.145 ± 0.017
$EW_{H\alpha}$ (Å)	77 ± 3	43 ± 5

extinction was also calculated using the FUV–NUV relations by Seibert et al. (2005). A more direct method of estimating A_{FUV}, using the ratio of the *IRAS* far-IR (FIR) flux with the FUV flux (Meurer, Heckman & Calzetti 1999), was also calculated for NGC 922. Both A_{FUV} values are comparable and equal 1.09 and 0.95 using the Seibert et al. (2005) and the Meurer et al. (1999) methods, respectively. This derived A_{FUV} is lower than most of the attenuations found in the local UV bright starburst galaxies (Meurer et al. 1999). *IRAS* data is not available for S2 and so the Seibert et al. (2005) method is used for both NGC 922 and S2.

The intrinsic fluxes [$f_0(\lambda)$], free from internal dust extinction, of NGC 922 and S2 were calculated from the observed fluxes [$f(\lambda)$] for the NUV, R, J, H and K measurements via

$$f_0(\lambda) = f(\lambda)10^{0.4E(B-V)_i k^e(\lambda)}, \quad (1)$$

where $E(B-V)_i$ is the reddening excess intrinsic to the galaxy which can be estimated using the relationships found in Calzetti, Kinney & Storchi-Bergmann (1994). The extinction relations for the stellar continuum [$k^e(\lambda)$] were calculated from the correlations determined by Calzetti et al. (2000). The intrinsic Hα fluxes were derived from the intrinsic R-band attenuation ($A_{R,i}$) from the adopted relation $A_{H\alpha,i} \approx 2A_{R,i}$ (Calzetti et al. 1994). A summary of foreground and internal extinction values in addition to the observed properties of NGC 922 and S2 from SINGG, SUNGG and 2MASS can be found in Table 1.

2.2 SFR, metallicity and mass

The star formation rate (SFR) was calculated by (i) using the Hα luminosity, $L_{H\alpha}$ (erg s^{-1}) (Kennicutt, Tamblyn & Congdon 1994):

$$SFR_{H\alpha} = \frac{L_{H\alpha}}{1.26 \times 10^{41}} \quad (2)$$

and (ii) using the FUV luminosity, L_{FUV} (erg s^{-1} Hz^{-1}) (Kennicutt 1998):

$$SFR_{FUV} = 1.4 \times 10^{-28} L_{FUV}. \quad (3)$$

The SFR calculated from method (i) for NGC 922 and S2 are 8.2 and 0.26 M$_\odot$ yr^{-1}, respectively. Similarly, the SFR calculated using the FUV luminosities for NGC 922 and S2 are 7.0 and 0.47 M$_\odot$ yr^{-1}, respectively.

The oxygen abundance [log(O/H) + 12] and metallicity (Z) can be approximated using the integrated flux ratios of various emission lines from the 6dF optical spectra. Within the wavelength range of

the 6dF spectra, it is possible to use the integrated flux ratios of the [N II] and [S II] emission lines as well as the flux ratios of [N II] and Hα (Kewley & Dopita 2002). The [N II]/[S II] = 1.12, 0.538 was measured for NGC 922 and S2, respectively. Assuming the average ionization parameter, $q = 2 \times 10^7$ cm s^{-1}, log (O/H) + 12 equals 9.0 and 8.6, respectively for NGC 922 and S2. These values indicate that the metallicity of NGC 922 is ∼1.0 Z$_\odot$ and the metallicity of S2 is ∼0.5 Z$_\odot$. Using the flux ratios of [N II]/Hα, log (O/H) + 12 equals 8.6 (∼0.5 Z$_\odot$) and 8.3 (∼0.3 Z$_\odot$) for NGC 922 and S2, respectively. Using the luminosity–metallicity relation found by Lamareille et al. (2004) for R-band luminosities in the local Universe, log (O/H) + 12 equals 9.1 and 8.3 for NGC 922 and S2, respectively. Both galaxies agree with the luminosity–metallicity relation.

The stellar mass ($M_\star$) of NGC 922 can be estimated using the K-band fluxes and the calibrations of Bell et al. (2003). Using this method, $M_\star$ is approximately 5.47×10^9 M$_\odot$ for NGC 922, while S2 has an order of magnitude less stars: $M_\star = 2.82 \times 10^8$ M$_\odot$, assuming it is a typical S0-Sa galaxy (as judged by its morphology) with $B - V$ colour of 0.8 (Sparke & Gallagher 2000). Assuming that the H I line profile is dominated by NGC 922 and its width gives the rotational velocity at the optical radius, one can estimate the enclosed dynamical mass using

$$M_{dyn}(R) = \frac{V_R^2 R}{G}, \quad (4)$$

where $V_R \approx 146$ km s^{-1} is the inclination corrected rotational velocity, the maximum radius of the R-band surface brightness profile $R = 13.4$ kpc and G is the gravitational constant. This yields a dynamical mass of 6.65×10^{10} M$_\odot$ within 13.4 kpc. The H I mass (M_{HI}) of NGC 922 was measured to be 1.2×10^{10} M$_\odot$ by HIPASS. We see that 8 per cent and 20 per cent of the dynamical mass of NGC 922 are due to the stellar and H I mass, respectively. It is probable from these calculations that most of the mass can be attributed to dark matter. The system is not in virial equilibrium and is expanding. This will mean that the total mass is probably an overestimation. As yet, the only H I observation of NGC 922 does not have enough spatial resolution to trace the neutral gas morphology of the system, hence, higher-resolution H I mapping of this system is needed to check if gaseous tails exist, such as the ones found in the Cartwheel galaxy (Higdon 1996). This would further verify our interacting companion. Table 2 summarizes the derived properties of both NGC 922 and S2.

3 ANALYSIS

Block et al. (2001) argue that the peculiar properties of NGC 922 mark it as a dust-obscured grand design spiral galaxy in the process of assembly, and hence it largely results from secular (interaction-free) evolution. Secular processes are indeed important in the present epoch (Kormendy & Kennicutt 2004) and can even produce ring like structures. However, in those cases the ring typically accompanies

Table 2. Derived properties of NGC 922 and S2.

Properties	NGC 922	S2
log (O/H) + 12	8.6–9.0	8.3–8.6
Z (Z$_\odot$)	0.5–1.0	0.3–0.5
SFR$_{H\alpha}$ (M$_\odot$ yr^{-1})	8.20 ± 0.32	0.26 ± 0.03
SFR$_{FUV}$ (M$_\odot$ yr^{-1})	7.04 ± 0.02	0.47 ± 0.02
$M_\star$ (M$_\odot$)	5.47×10^9	2.82×10^8
M_{dyn} (M$_\odot$)	6.65×10^{10}	−
M_{HI} (M$_\odot$)	1.2×10^{10}	−

a strong bar producing a θ morphology, quite different from what is observed in NGC 922. While some aspects of the morphology of NGC 922 may have a secular origin, the observed evidence for a strong interaction is very compelling.

We propose that the outstanding properties of NGC 922 are likely to be the result of a high-speed, off-centre collision between a gas-rich disc galaxy and a dwarf companion for the following reasons. (1) The stellar plume observed in NGC 922 extending towards S2 is most likely to be caused by an external mechanism such as the tidal interaction between NGC 922 and its companion galaxy. (2) Numerous simulations (e.g. Hernquist & Weil 1993) have shown that ring structures can be formed from outwardly propagating waves. (3) From our observations of the flocculent region in between the centre and the ring of NGC 922, the 'arms' of the inner spiral observed by Block et al. (2001) can be described as 'spoke'-like structures analogous to those observed in the Cartwheel galaxy. (4) The high SFR and EW of NGC 922 and S2, coupled with the low gas cycling time of the system indicates a recent starburst. We are aware that this reason alone does not necessarily rule out a secular origin for the global properties of NGC 922 since starbursts have been observed in systems with no obvious companions (e.g. Meurer et al. 1996). Similarly, simulations show that if a bar or disc can be displaced from the centre of mass in a galaxy, lopsided arms or a single arm can result in a morphology similar to the partial ring of NGC 922, although an external perturbation still may be needed to excite the offset (Colin & Athanassoula 1989; Bournaud et al. 2005).

Although secular evolution may account for some of the observed properties of NGC 922, we find that *all* the observed features of NGC 922 can be explained by a high-speed, off-centre collision between a gas-rich spiral and a dwarf, which we model below. Since our main focus is on the observed properties of NGC 922, rather than the details of the simulation results for a range of model parameters, we present only the results for which the observed morphology can be reproduced reasonably well. Detailed descriptions of the numerical methods and techniques used to model the dynamical evolution of interacting galaxies can be found in Bekki et al. (2002).

3.1 Model and simulations

NGC 922 and S2 are represented by a self-consistent disc galaxy model and a point mass, respectively. The progenitor disc galaxy of NGC 922 consists of a dark halo and a thin exponential disc. The masses and distances are measured in units of total disc mass (M_d) and total disc size (R_d). Velocity and time are measured in units of $v = (GM_d/R_d)^{1/2}$ and $t_{dyn} = (R_d^3/GM_d)^{1/2}$, respectively. The units are scaled so that $G = 1.0$. The radial (R) and vertical (Z) density profiles of the disc are assumed to be proportional to $\exp(-R/R_0)$ with scalelength $R_0 = 0.2$ and to $\mathrm{sech}^2(Z/Z_0)$ with scalelength $Z_0 = 0.04$ in our units, respectively. The initial radial and azimuthal velocity dispersions are added to the disc component in accordance with epicyclic theory, and a Toomre parameter value of $Q = 1.5$ (Binney & Tremaine 1987).

The vertical velocity dispersion at a given radius is proportionally half the radial velocity dispersion such as observed in the Milky Way (e.g. Wielen 1977). Assuming that $M_d = 2.0 \times 10^{10}\,\mathrm{M_\odot}$ and $R_d = 13.4$ kpc for the disc galaxy; $v = 80.1\,\mathrm{km\,s^{-1}}$, $t_{dyn} = 164$ Myr, radial scalelength of the disc equals 2.68 kpc and the maximum rotational velocity equals $145\,\mathrm{km\,s^{-1}}$. The total mass of NGC 922 enclosed within R_d is $7.5 \times 10^{10}\,\mathrm{M_\odot}$. The gas mass fraction of the spiral is assumed to be 0.2 and the Schmidt law (Schmidt 1959) with an

index of 1.5 (Kennicutt 1989) is adopted for star formation in the disc galaxy.

The assumed mass ratio between the dwarf companion and the spiral is 0.2. X_g and V_g represents the initial locations and velocities of the companion with respect to the centre of the disc galaxy. For the model presented here, $X_g = (x, y, z) = (-4R_d, 0.5\,R_d, 0)$ and $V_g = (v_x, v_y, v_z) = (6v, 0, 0)$. The inclination of the spiral with respect to the xy plane is assumed to be $80°$, hence the xy plane roughly corresponds to the tangential plane of our images. The adopted values of $v_x = 6v$ (corresponding to the relative velocity of $\sim 481\,\mathrm{km\,s^{-1}}$) and $y = 0.5R_d$ (~ 6.7 kpc) represents an off-centre very high-speed collision. Note that stars that are initially within the disc of the spiral are referred to as 'stars' (or 'old stars'), while the stars that are formed after the collision from the gas are referred to as 'new stars'.

3.2 Results

Fig. 3 describes how a ring galaxy is formed during an off-centre collision between a spiral and its dwarf companion. The rapid passage of the companion through the disc initially causes the disc to contract as it feels the mass of the companion and then to expand as the mass disappears, resulting in an expanding density wave (Lynds & Toomre (1976); Hernquist & Weil (1993)). Within 0.2 Gyr of the spiral–dwarf collision, a non-axisymmetric ring-like structure and a tidal plume composed mainly of gas and old stars are formed. Owing to the strong compression of the disc gas, new stars have formed along the C-shaped ring.

In comparison to our observations, the observed morphology of NGC 922 is best matched by the simulated model at 0.33 Gyr after the collision. At $T = 0.33$ Gyr, the radius of the ring is ~ 14–15 kpc and the distance between the simulated disc galaxy and its companion is ~ 104 kpc. These values are comparable to both the observed radius of NGC 922 and the projected distance between NGC 922 and S2.

In Fig. 3, the companion is no longer visible at $T = 0.33$ Gyr due to its high relative velocity, while $v_z(T = 0.33) \sim 203\,\mathrm{km\,s^{-1}}$ of the intruder is in reasonable agreement with the radial velocity
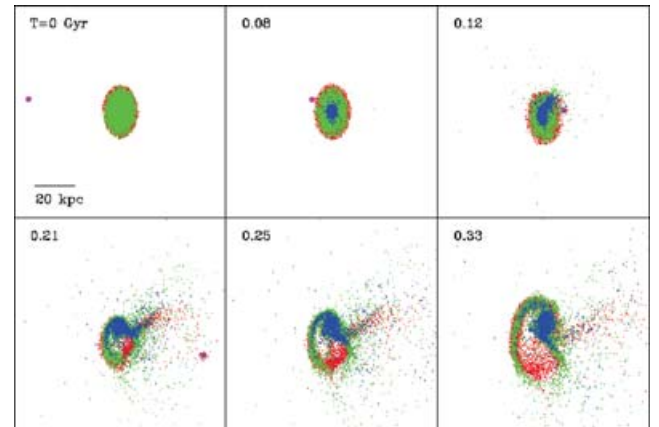
Figure 3. Morphological evolution of a gas-rich, bulgeless spiral colliding with a dwarf companion (represented by a big pink dot). Time (T) in Gyr since the start of the simulation is shown in the upper left-hand corner of each panel. Stars, gas and new stars are shown in green, red and blue, respectively. For clarity, dark matter particles are not shown. The companion comes from the left-hand side and passes through the central region of the spiral. Note that the simulated 'C-shaped' morphology is strikingly similar to the observed morphological properties of NGC 922.

difference between NGC 922 and S2. In conclusion, the observed ring morphology of NGC 922 can be reproduced simply by passing a point mass through a disc galaxy as shown above.

4 CONCLUSIONS

Block et al. (2001) showed that the structure of NGC 922 determined from Fourier decomposition of IR images is similar to that of grand-design spirals, which are presumably evolving in a secular fashion. Hence the dominant galaxy may originally have been a spiral. However, concentrating on the IR properties minimizes the significance of the star formation event which is well traced by our Hα and UV observations. These show a very disturbed morphology. The most compelling argument for a drop through encounter in the NGC 922 system is the ease in which this scenario can account for all the major features of the system: the off-centre star forming bar, a nearly complete star forming ring, the low-mass companion and the plume of stars apparently directed at the companion. We are not aware of any self-consistent secular models which also produce all these features.

Although ring or ring-like galaxies only account for 0.02–0.2 per cent of all spiral galaxies (Athanassoula & Bosma 1985) in the local Universe, they should be more common at higher redshifts, since both galaxy density and the dispersion about the Hubble flow increase with redshift. C-shaped rings like that in NGC 922 should be more common at all redshifts than complete rings like the Cartwheel galaxy, since off-axis collisions are more likely than on-axis ones. Indeed, five out of the eight example high redshift *clump cluster* galaxies shown by Elmegreen et al. (2005) have a ring or partial ring morphology.

Our observations and simulations demonstrate that the ring galaxy NGC 922 can be formed by the slightly off-axis passage of a dwarf companion through the disc of a spiral galaxy. A series of expanding density waves consisting of both stellar and gaseous material result from the collision and enhanced star formation in the ring and the core of NGC 922 (due to the compression of the displaced gas) is observed. We are not able to discuss the star formation induced in the companion from these simulations since we simply modelled the companion as a point mass. In the future, more sophisticated simulations could probe the star formation scenario and stellar populations of the companion, while H I synthesis observations of the system could check for the existence of a gaseous tail between NGC 922 and S2.

REFERENCES

Athanassoula E., Bosma A., 1985, ARA&A, 23, 147
Bekki K., Forbes D. A., Beasley M. A., Couch W. J., 2002, MNRAS, 335, 1176
Bell E. F., McIntosh D. H., Katz N., Weinberg M. D., 2003, ApJS, 149, 289
Binney J., Tremaine S., 1987, Galactic Dynamics. Princeton Univ. Press, Princeton, NJ, p. 747
Block D. L., Puerari I., Takamiya M., Abraham R., Stockton A., Robson I., Holland W., 2001, A&A, 371, 393
Bournaud F., Combes F., Jog C. J., Puerari I., 2005, A&A, 438, 507
Calzetti D., Kinney A. L., Storchi-Bergmann T., 1994, ApJ, 429, 582
Calzetti D., Armus L., Bohlin R. C., Kinney A. L., Koornneef J., Storchi-Bergmann T., 2000, ApJ, 533, 682
Colin J., Athanassoula E., 1989, A&A, 214, 99
Elmegreen D. M., Elmegreen B. G., Rubin D. S., Schaffer M. A., 2005, ApJ, 631, 85
Hernquist L., Weil M. L., 1993, MNRAS, 261, 804
Higdon J. L., 1996, ApJ, 467, 241
Jarrett T. H., Chester T., Cutri R., Schneider S., Skrutskie M., Huchra J. P., 2000, AJ, 119, 2498
Jones D. H., Saunders W., Colless M., Read M. A., Parker Q. A., Watson F. G., Campbell L. A. et al., 2004, MNRAS, 355, 747
Kennicutt R. C., 1989, ApJ, 344, 685
Kennicutt R. C., 1998, ARA&A, 36, 189
Kennicutt R. C., Tamblyn P., Congdon C. E., 1994, ApJ, 435, 22
Kewley L. J., Dopita M. A., 2002, ApJS, 142, 35
Koribalski B. S., Staveley-Smith L., Kilborn V. A., Ryder S. D., Kraan-Korteweg R. C., Ryan-Weber E. V., Ekers R. D. et al., 2004, AJ, 128, 16
Kormendy J., Kennicutt R. C., 2004, ARA&A, 42, 603
Lamareille F., Mouhcine M., Contini T., Lewis I., Maddox S., 2004, MNRAS, 350, 396
Lynds R., Toomre A., 1976, ApJ, 209, 382
Meurer G. R., Carignan C., Beaulieu S. F., Freeman K. C., 1996, AJ, 111, 1551
Meurer G. R., Heckman T. M., Calzetti D., 1999, ApJ, 521, 64
Meurer G. R., Hanish D., Ferguson H. C., Knezek P. M., Kilborn V. A., Putman M. E., Smith R. C. et al., 2006, ApJ, in press
Meyer M. J., Zwaan M. A., Webster R. L., Staveley-Smith L., Ryan-Weber E., Drinkwater M. J., Barnes D. G. et al., 2004, MNRAS, 350, 1195
Mould J. R., Huchra J. P., Freedman W. L., Kennicutt R. C., Ferrarese L., Ford H. C., Gibson B. K. et al., 2000, ApJ, 529, 786
Schlegel D. J., Finkbeiner D. P., Davis M., 1998, ApJ, 500, 525
Schmidt M., 1959, ApJ, 129, 243
Seibert M. et al., 2005, ApJ, 619, L55
Sparke L. S., Gallagher J. S., 2000, in Linda S. Sparke, John S. Gallagher III, eds, Galaxies in the Universe: An Introduction. Cambridge Univ. Press, Cambridge, p. 416, ISBN 0521592410
Wielen R., 1977, A&A, 60, 263

This paper has been typeset from a TEX/LATEX file prepared by the author.